Numerical analyses of the earthquake-induced Takanodai landslide, Kumamoto, Japan

Gabriele Chiaro [i], Kevin S.Y. Chew [ii] and Joon-Su Kim [iii]

i) Senior Lecturer, Department of Civil and Natural Resources Engineering, University of Canterbury, Private Bag 4800, Christchurch 8140, New Zealand; Email: gabriele.chiaro@canterbury.ac.nz
ii) Formerly, Student, Dept. of Civil and Natural Resources Engineering, University of Canterbury, Private Bag 4800, Christchurch 8140, New Zealand; Geotechnical Engineer, Beca Ltd., Aorangi House, 85 Molesworth Street, Wellington 6011, New Zealand
iii) Formerly, Student, Dept. of Civil and Natural Resources Engineering, University of Canterbury, Private Bag 4800, Christchurch 8041, New Zealand; Geotechnical Engineer, Golder Associates (NZ) Ltd., 214 Durham Street, Christchurch 8011, New Zealand.

ABSTRACT

The 2016 Kumamoto Earthquakes, Japan, caused a number of geo-disasters in the Aso Volcanic Caldera, including a large-scale flow-type slope failure known as the Takanodai landslide. Between April and October 2016, the First Author conducted a series of post-earthquake geotechnical damage surveys and field investigations in the affected areas, and retrieved samples of volcanic soils. Following a detailed laboratory soil characterization, a numerical investigation including dynamic soil response and seismic slope stability analyses were performed by using the Quake/W and Slope/W software. In this paper, the results of the numerical analyses are presented and discussed. The numerical investigation indicated that the pumice soil deposit was responsible for the landslide triggering, and that the key factors for the flow-type failure were a combination of large inertial forces (i.e. shear stresses) and significant excess pore water pressure generation.

Keywords: volcanic soils, Takanodai landslide, dynamic slope response, seismic slope stability analysis

1 INTRODUCTION

On 16 April 2016, a moment magnitude (M_w) 7.0 earthquake struck the Island of Kyushu, Japan. It was preceded by two major foreshocks of M_w 6.2 (14 April) and M_w 6.0 (15 April). The earthquake sequence contributed to devastation in the mountainous areas of the Aso Caldera, where medium to large scale landslides and rock falls were frequently observed. Among these, the earthquakes caused the failure of a gentle slope near the Aso Volcanological Laboratory in Minami Aso Village (Dang et al., 2016; Kiyota et al, 2016; Mukunoki et al., 2016; Chiaro et al., 2017a). This large-scale runout slope failure, known as the Takanodai landslide, destroyed at least 7 houses of the Takanodai Housing Complex, killed 5 people, threatened many other houses and blocked several roads (Fig. 1).

The Kumamoto Prefectural Government designated residential landslide hazard zones using the following criteria: (1) steep areas at least 5 m high with a slope of 30º or more, (2) areas below a rapid mountain stream that has formed as alluvial fan, and (3) areas where landslides have occurred or are at risk of occurring. The Takanodai Housing Complex slope feature did not meet any of these national criteria. Therefore, it was not classified as a potential seismic hazard under the national standards for landslide prevention (Dang et al., 2016).

Between April and October 2016, as a part of the NZSEE LFE Kumamoto Mission and J-Rapid Japan-NZ Kumamoto Project, the First Author conducted a series of geotechnical damage surveys and field investigations in the Aso Caldera, and retrieved samples of volcanic soils at the Takanodai site to be characterized in the laboratory. One of the primary objectives of this research effort was to provide in-depth understandings into the failure mechanism of the Takanodai landslide and evaluate the liquefaction potential of the Aso pumice believed to be the key soil responsible for the activation of the landslide.

Initial field observations suggested that the key soil to cause the slope failure could be the orange-colored pumice soil deposit (Mukunoki et al., 2016; Chiaro et al., 2017a). Moreover, the sensitivity ratio of shear strength of this volcanic soil before and after the earthquake as well as the water pressure buildup could be the cause for the flow type slope failure. Hence, further site investigations and in-depth experimental and numerical studies were required to clarify the mechanisms for such a flow-type failure of the Takanodai gentle slopes.

Following a detailed laboratory soil characterization (Umar et al., 2017, 2018; Chiaro et al., 2018), a

numerical investigation including dynamic soil response and seismic slope stability analyses was performed by using the Quake/W (Quake/W, 2014) and Slope/W (Slope/W, 2012) software. In this paper, the results of the numerical analyses are presented and discussed.

2 FIELD OBSERVATIONS

2.1 Takanodai landslide characteristics

Field observations indicated that the Takanodai landslide was a mobile earth slide that developed into a flow-type slide on a low angle slope (around 10-15º), with a travel angle from landslide crown to debris toe of approximately 6º (Fig. 1b). The landslide moved in three different directions from a common source (Fig. 1a). It was about 100 m in width, 300-600 m in length and 5-10 m in depth.

As shown in Fig. 2, relatively large intact blocks of soil, grass and trees travelled towards the toe of the slope suggesting a translational movement of the soil. Tension cracks above the head scarp adjacent the Aso Volcanological Laboratory were commonly observed, indicating the potential for head scarp retrogression and/or new incipient landslides to occur. Fig. 2d shows the identified slip surface and traces of orange-colored pumice soil that were noted on it.

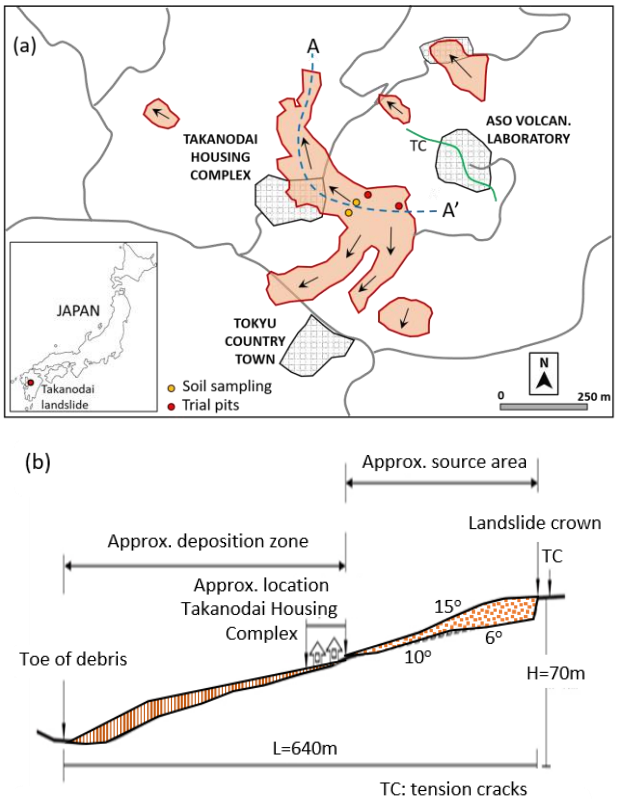

Figure 1. (a) Plan view of the Takanodai landslide (adopted from Chiaro et al., 2017a); and (b) Cross-section A-A' through the Takanodai landslide.

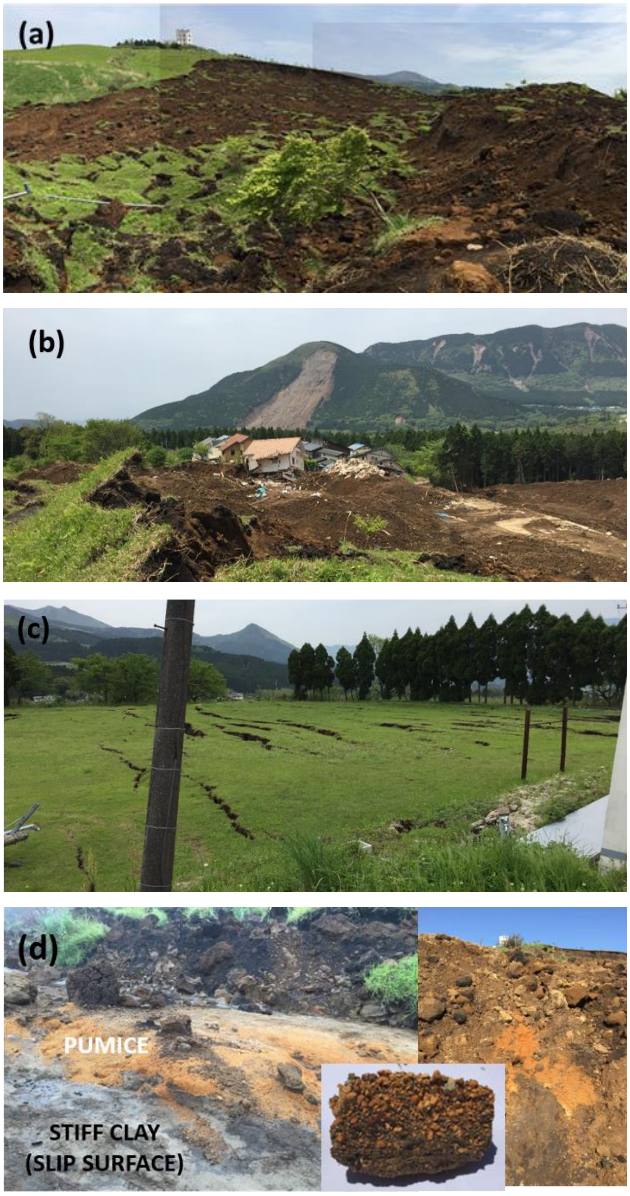

Figure 2. View of the Takanodai landslide: (a) looking uphill, with the Aso Volcanological Laboratory visible in the distance; (b) looking downhill, with the destroyed Takanodai Housing Complex; (c) tension cracks at the Aso Volcanological Laboratory; (d) traces of orange pumice soil on the identified slip surface (photos taken in May 2016).

2.3 Soil sampling

Undisturbed and disturbed samples of Aso pumice soils were retrieved to be characterized in the laboratory (Umar et al, 2017 and 2018; Chiaro et al., 2018). Moreover, two small trial pits were excavated across the slip surface (see the location in Figure 1).

Soil exposed in the trial pit is shown in Fig. 3. The soil consists of: (1) Kuroboku clay-like volcanic soil with organic contents (black color); (2) Akaboku clay-like volcanic soil (red/brown color); (3) pumice soil (orange color); and (4) soft/weathered rock.

It should be noted that, the Akaboku volcanic soil (clay-like soil), within which the pumice soil is sandwiched, is a much less permeable soil deposit than the pumice one. Moreover, water seepage was clearly observed within the pumice soil layer during the field survey. This would imply that, the pumice soil was most likely fully saturated at the time of the earthquake(s).

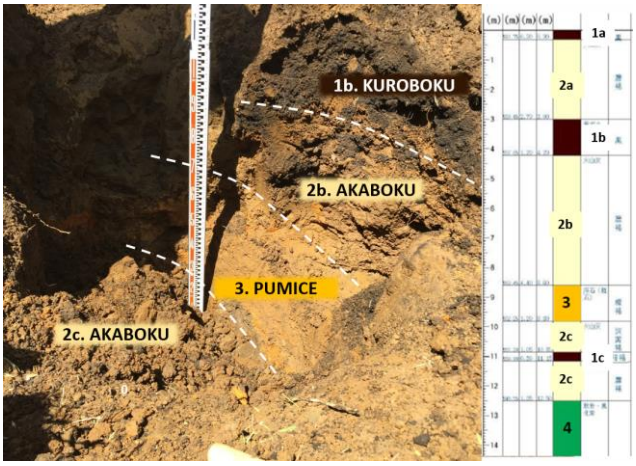

Figure 3. Soils exposed in wall of a trial pit excavated in the northern flank of the landslide (photos taken in May 2016). The borehole data were retrieved from: http://geonews.zenchiren.or.jp/api/2016KumamotoEQ/index.htlm

3 NUMERICAL MODEL

3.1 Soil model and slope geometry

The Takanodai landslide can be classified as earth/debris flow, which is a relatively fluid and rapid type of landslide. Field observations and subsequent laboratory investigations also indicated that the key soil material in which the slide surface developed was most likely the pumice, which was saturated at the time of the field visit. On this basis, earthquake-induced liquefaction of the Aso pumice (i.e. failure through the pumice soil deposit) was hypothesized to be the key triggering mechanism for the assessed damaged areas.

To confirm the validity of this assumption, a two-dimensional (2-D) numerical model of the Takanodai landslide was created based on the slope geometry shown in Fig. 1b and the typical soil profile shown in Figs. 3 and 4. The numerical model was implemented into Quake/W software to evaluate the dynamic soil response. Then, Slope/W software was used to evaluate (i.e. back-analyze) the seismic slope stability of the Takanodai slope. Note that, the equivalent linear soil behavior model was used for the assessment (Kramer, 1996), while pore water pressure generation (PWP) was enabled.

The success of a geotechnical numerical model highly depends on the accuracy of material properties defined by the user, namely soil stiffness, soil strength parameters, density, damping ratio, liquefaction triggering curve and pore water pressure generation. For a dynamic analysis of this kind, the shear modulus (G) needs to be specified and how the pore-pressure is affected by cyclic stress needs to be addressed. The soil's ability to dissipate energy in the form of damping induced by the earthquake motions was a critical factor to consider as well.

As an initial verification measure that the Quake/W model had no convergence problems, the material models were assumed to behave in a linear-elastic manner. Once sufficient confidence for the soil parameters was gained through the linear-elastic model, equivalent linear model was then implemented. Quake/W permits the simulation of nonlinear behavior of soils using the equivalent linear analysis. This analysis method allows for more accurate computation of the soil behavior through a dynamic analysis with the specified soil stiffness. The Quake/W software identifies the maximum shear strains at each Gauss numerical integration point in each element and the shear modulus is modified according to the specified G reduction function for the particular soil type. This process is repeated until the convergence has been achieved within the specified tolerance. One notable feature of the model is that the G value is a constant during one iterative step through the earthquake record but it is adjusted between the subsequent steps through the record. Hence, the maximum shear modulus (G_{max}) for the soil needs to be defined with reasonable accuracy for the first calculation step of the equivalent linear analysis.

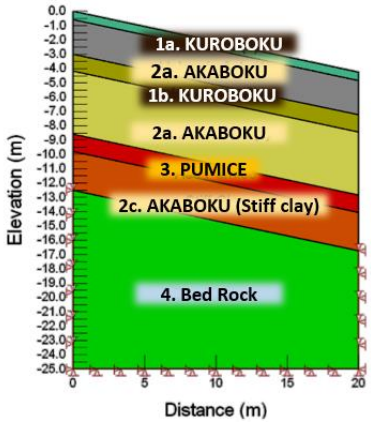

Figure 4. Soil profile used in the numerical analysis.

3.2 Dynamic response and seismic slope stability

The dynamic stress response obtained by Quake/W was examined using Slope/W Newmark function to compute the stability of the slope subjected to earthquake shaking (Slope/W, 2012).

For each trial slide surface, Slope/W uses: 1) the initial lithostatic stress condition to establish the static strength of the slope (i.e., the static factor of safety); and 2) the dynamic stress (from Quake/W) at each time step to compute the dynamic shear stress of the slope and the factor of safety (FoS) at each time step during the modelled earthquake. Slope/W determines the total

mobilized shear arising from the dynamic inertial forces. The dynamically driven mobilized shear force is then divided by the total slide mass to obtain an average acceleration for a given slide surface at a given time step. The acceleration response for the entire potential sliding mass represents the acceleration value that affects the stability at a given time step during the earthquake.

The soil properties used for the Slope/W assessment are summarized in Table 1.

Table 1. Soil properties used in the numerical analyses.

Layer	Soil type	Bulk unit weight (kN/m^3)	G_{max} (MPa)	Cohesion (kPa)	Friction angle (^{o})
1a	Kuroboku	11.2	27	15.3	23.7
2a	Akaboku	12.9	27	15.3	23.7
1b	Kuroboku	11.2	27	15.3	23.7
2b	Akaboku	19.2	35	15.3	23.7
3	Pumice	11.3	50	0	40
2c	Akaboku (stiff clay)	19.2	100	150	23.7
4	Soft Rock	22.0	450	-	-

3.3 Input ground motions

The earthquakes considered were the 14 April (M_w 6.2) and 16 April (M_w 7.0) events. To account for any possible volcanic basin effects, the E-W horizontal acceleration components from the strong motion station KMM007 (Fig. 5) – located within the Aso Volcanic Caldera - were used.

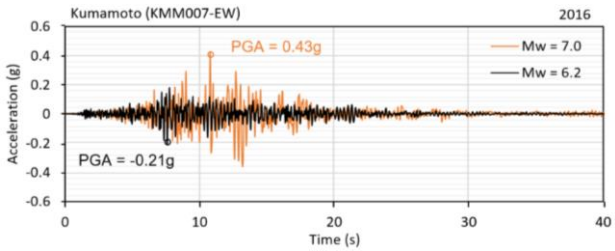

Figure 5. E-W acceleration records from KMM007 ground motion station (http://www.kyoshin.bosai.go.jp/) used in the numerical Quake/W-Slope/W analysis.

4 SOIL MODEL PARAMETERS

The strain-dependent shear-modulus reduction and damping functions for the rock materials and clayey deposits were defined from the literature for similar volcanic soils (e.g. Meyer et al., 2005). Compression (V_p) and shear (V_s) wave velocities from borehole logs at the Mashiki Town allowed for the estimation of the stiffness of the stiff clay and bedrock layers. Then, combining the adopted V_s measurements with the actual soil density, the small-strain shear moduli (G_{max}) were estimated (Table 1).

Model parameters for the Aso pumice, including the PWP function, were obtained from the analysis of the test results presented in Umar et al. (2017, 2018) and Chiaro et al. (2018).

The accurate definition of the soil properties is an important geotechnical earthquake consideration. The unit weight of the materials was obtained from the site investigations conducted at Takanodai landslide site. Poisson's ratio of 0.25 ($K_0 \approx 0.5$) was assumed for all volcanic soils investigated.

4.1 Pore-pressure ratio function

Under intense ground shaking, build-up of excess pore water pressure can lead to significant loss of soil strength and stiffness, ultimately causing liquefaction.

This effect was modelled in Quake/W using a pore-pressure ratio function defined by the cyclic number ratio (N/N_L) and the pore water pressure ratio (r_u). Experimental results from undrained cyclic torsional simple shear test on Aso Pumice reported in Umar et al. (2017, 2018) and Chiaro et al. (2018) were used to define the ratio function shown in Fig. 6. The experimental data showed a similar trend to the pore-pressure ratio function defined empirically by Lee and Albaisa (1974), implemented in Quake/W, hence providing a degree of confidence in the data.

Note that, due to very low liquefaction potential, a pore-water pressure function was not defined for the clay-like volcanic soils.

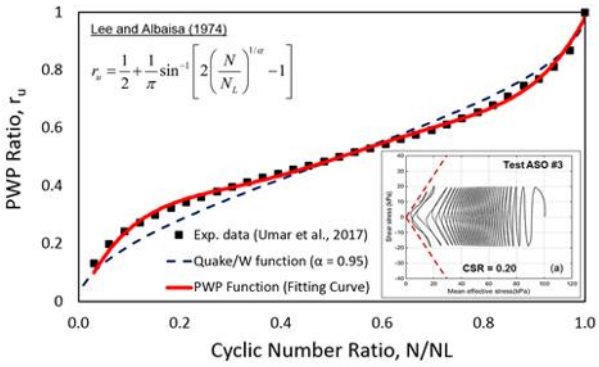

Figure 6. Pore-pressure ratio function for Aso Pumice.

4.2 Cyclic resistance curve

The cyclic resistance curve supplements the pore-pressure ratio function by computing the cyclic stress ratio to produce initial liquefaction for a given number of equivalent uniform cycles (Seed and Idriss, 1971). Experiment results from Umar et al. (2017) and Chiaro et al. (2018) combined with the predefined functions from Quake/W showed that the Aso Pumice cyclic behavior closely resembled that of a medium loose sand (Fig. 7).

4.3 Critical state strength

When soil liquefies under large shear strains, its strength parameters will diminish to a residual strength. The Quake/W and Slope/W analyses quantify this behavior via a critical state strength (CSS) and a collapse surface angle. For Aso pumice, the CSS was found to be 34 kPa from the laboratory test by Chiaro et al. (2018), while the collapse surface angle was taken as

two-thirds of the effective friction angle as recommended by Kramer (1996).

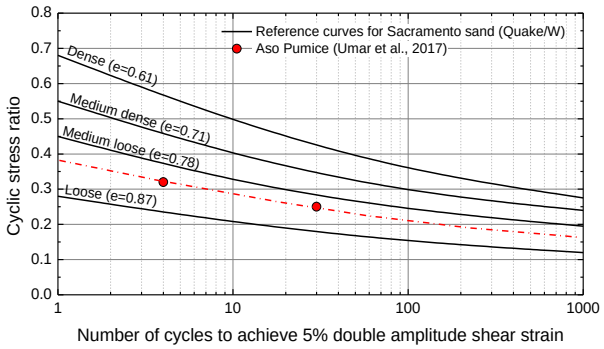

Figure 7. Cyclic shear strength of Aso Pumice

4.4 Dynamic soil properties

Uppermost clay-like volcanic soils. Due to the absence of experimental data (at the time of writing this paper) for the Kuroboku and Akaboku clay-like volcanic soils found at Takanodai investigation site, the dynamic properties of the clay-like uppermost soil deposits were modelled using data of a similar clay-like volcanic soil typically found in the North Island of New Zealand, namely Tauranga Clay.

Meyer et al. (2005) conducted bender element and free vibration torsion testing on high quality Tauranga Clay samples to determine the shear modulus reduction and damping ratio curves, which were adopted in this study for use in the Quake/W soil model (Fig. 8).

Aso pumice. The dynamic properties of Aso Pumice are shown in Fig. 9. They were obtained from the experimental data presented by Umar et al. (2017).

Stiff clay beneath the pumice layer. Due to the absence of experimental data (at the time of writing this paper) for the Akaboku stiff clay layer, it was assumed that the stiff clay found in Mashiki Town could be a good representation of the stiff clay found at the landslide site due to its close proximity to the damaged site of interest and similar geological age. For this reason, the borehole records presented by Goto et al. (2017) were adopted to determine the dynamic properties of the stiff clay used in the model (Fig. 10).

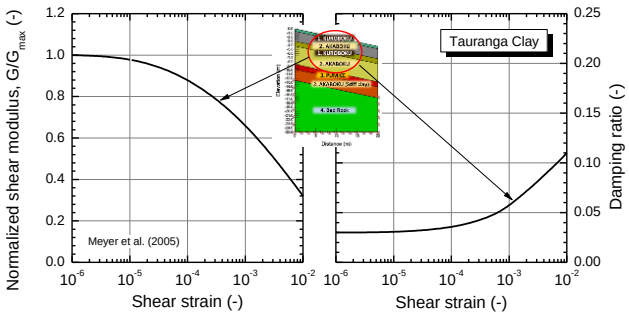

Figure 8. Dynamic properties adopted for Kuroboku and Akaboku clay-like volcanic soils.

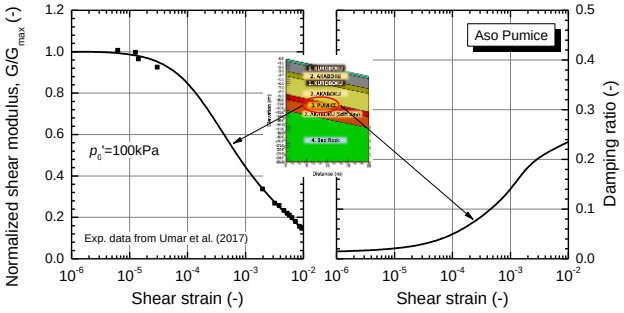

Figure 9. Dynamic properties of Aso Pumice.

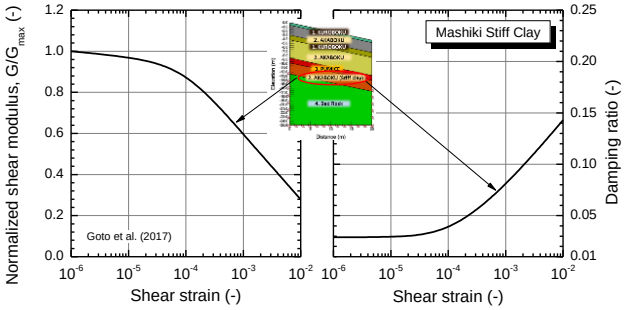

Figure 10. Dynamic properties of Mashiki stiff clay (Goto et al., 2017) used to model the Akaboku stiff clay layer.

5 NUMERICAL ANALYSIS RESULTS

In this paper, the behavior of the Takanodai landslide was investigated under both static and seismic conditions.

5.1 Static slope stability analysis

As shown in Fig. 11, the static analysis indicated that the pre-quake slope configuration at the Takanodai Housing Complex was highly stable, having a minimum factor of safety (FoS) of 3.

5.2 Seismic slope stability analyses

Mw 6.2 (14 April 2016): fore-shock. The downslope direction of the Takanodai Housing Complex hill faces the North-West direction. With both N-S and E-W ground motion records available, the ground motion with a larger amplitude (E-W) was chosen as the predominant direction of shaking for the dynamic analysis. This meant that any difficulties arising from the earthquake directionality effects could be mitigated up to certain extent. The seismic motion in the E-W direction recorded at KMM007 station was characterized by a peak ground acceleration (PGA) of 0.21g at about 7 seconds (see Fig. 6).

Figure 11 illustrates the variation of sesmic factor of safety (FoS) values with time for the dynamic analysis using the foreshock event records. While most of the FoS values were well above 1.0, it was observed that FoS dropped to a value of just above 1.0 at approximately 7 seconds, in correspondence of the PGA. However, a close look at the critical slip surface revealed the occurrence of only a local shallow failure in correspondence of the crest of the slope.

Mw 7.0 (16 April 2016): main-shock. Similarly to the foreshock event, the E-W component of the main-shock acceleration record was selected for the analysis. In this case the PGA = 0.43g.

The FoS values for the main-shock analysis suggests the initiation of global failure for the slope occurring at approximately 9-10 seconds (Fig. 11a), well before the actual PGA occurred at 12 seconds. Specifically, the FoS dropped to a value of 0.79 (green circle in Fig. 11a). As shown in Fig. 11b, the critical slip surface closely resembled the failure observed at the Takanodai landslide site (Fig. 1b).

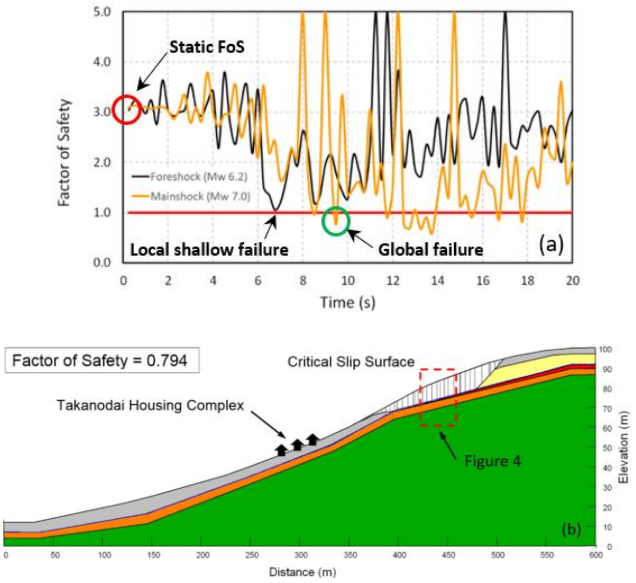

Figure 11. (a) Static and dynamic factor of safety (FoS) for the Takanodai Housing Complex hillslope during the foreshock and main-shock events; and (b) Critical slip surface during the main-shock

6 POTENTIAL FAILURE MECHANISMS

Based on the field observations, dynamic analyses presented here and experimental tests results reported in detail in Chiaro et al. (2018), two possible flow-type failure mechanisms can be envisioned for the Takanodai landslide, as described below.

6.1 Type I: abrupt flow-type failure

This failure mode would imply that the main earthquake generated dynamic shear stresses so high that the peak shear strength of the pumice layer was exceeded during the seismic event. In addition, a partial but significant build-up of pore water pressure took place within the pumice layer. This would have resulted in a flow-type failure mechanism similar to that revealed by the monotonic test ASO#2 shown in Fig. 12, characterized by an abrupt development of large shear strain within the weak pumice layer.

6.2 Type II: liquefaction-induced flow-type failure

This failure mode would involve a substantial build-up of pore water pressure occurred within the pumice layer during the seismic shaking, leading to a drastic reduction of stiffness and strength of the pumice layer due to soil fluidization or liquefaction. This phase would have been then followed by a flow-type failure involving a sudden development of extremely large strains, as described by the cyclic test ASO#4 shown in Fig. 13.

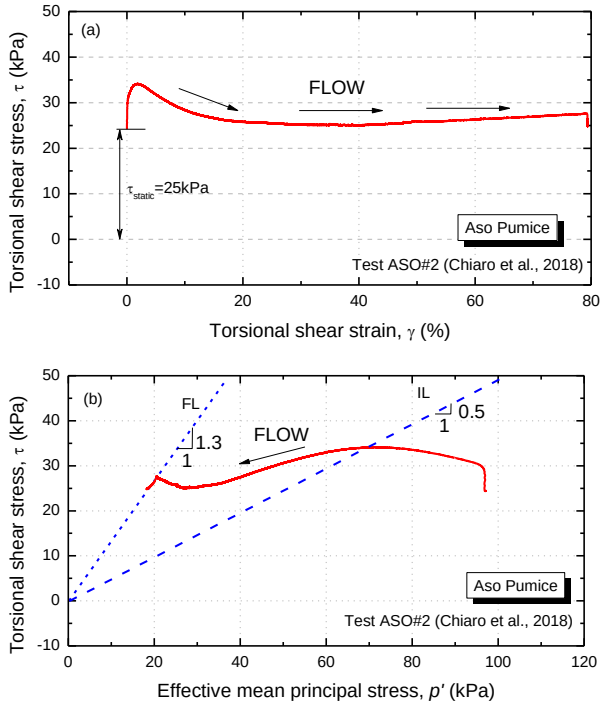

Figure 12. Monotonic undrained torsional simple shear behavior of Aso Pumice subjected to initial static shear: (a) stress-strain relationship; and (b) effective stress path (Chiaro et al., 2018).

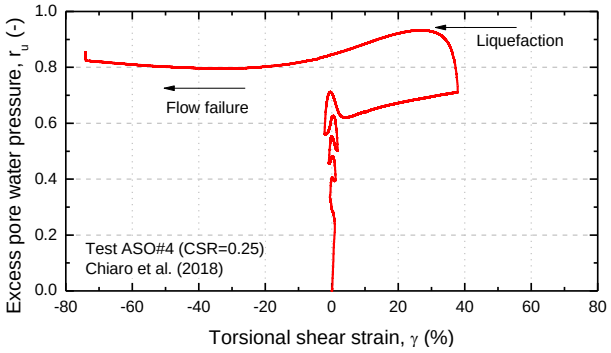

Figure 13. Cyclic undrained torsional simple shear behavior of Aso Pumice (Chiaro et al., 2018).

8 DISCUSSIONS

8.1 Landslide hazard criteria

As reported by Dang et al. (2016), the Kumamoto prefectural government had created "landslide hazard maps" based on national standards for landslide prevention based on three criteria (refer to Introduction). The slopes surrounding the Takanodai Housing Complex did not meet any of these criteria and, thus, were not included in the landslide hazard maps.

These criteria, however, are merely based on consideration of slope geometry, geomorphology features and evidence of past slope failure. They do not account explicitly for the presence or not of problematic soil deposits (i.e. liquefiable and/or crushable volcanic soils), the thickness of such challenging volcanic deposits and the depth from ground surface of critical layers. As shown by this study, if well-planned field investigations, laboratory tests and numerical dynamic analyses (accounting for slope geometry, actual soil profile and soil properties, liquefaction potential of volcanic soils) are used, dangerous slopes similar to that of Takanodai one, could be identified and, therefore, improved earthquake-induced landslide hazard maps in volcanic areas could be obtained.

8.2 In-depth understanding of cyclic behavior of volcanic soils

Worldwide, large-magnitude earthquakes (M_w>7) usually trigger a large number of slope failure in mountainous areas (Yin et al., 2009; Chiaro et al., 2015; Dellow at al., 2017). However, earthquake-induced slope failures in volcanic areas are of major concern due to the presence of problematic volcanic soils (Yamanouchi, 1968; Ishihara and Harada, 1996; Chigira and Suzuki, 2016; Wang, 2017).

Nevertheless, to date, very limited research has been undertaken to comprehensively understand the cyclic undrained behavior of challenging volcanic soils and their failure mechanisms. In addition, due to peculiar properties, such as high crushability and compressibility, high internal void ratio (Hyodo et al., 1998; Wesley, 2001; Pender at al., 2006; Asadi et al., 2018), existing correlating to estimate the liquefaction characteristics of hard grained (less crushable) soils are not applicable to highly crushable volcanic soils. Therefore, it is essential to conduct comprehensive investigations that enable the understanding of typical failure mechanisms of volcanic soil under cyclic shear loading and establishment of soil-specific liquefaction criteria suitable for this problematic soils.

9 CONCLUSIONS

Following reconnaissance damage surveys, a thin deposit of crushable pumice soil was understood to be responsible for the Takanodai landslide occurred in Minami Aso during the 2016 Kumamoto earthquakes. However, there were debates in regard to the potential failure mechanisms among researchers. To provide insights into the failure mechanisms of the Takanodai landslide, well-organized field investigations, advanced laboratory tests and numerical analyses were carried out by the Authors.

In this paper, the results of a numerical investigation including dynamic soil response and seismic slope stability analyses performed by using the Quake/W and Slope/W software were presented and discussed. The following main conclusions can be drawn from this study:

1) The dynamic soil response and seismic slope stability analyses confirmed that Aso pumice layer was responsible of the activation of the Takanodai landslide (i.e. failure developed within the pumice soil layer). The factor of safety under static conditions was approximately 3 and dropped to a values of less than 0.8 during the main earthquake shaking event.
2) No failure was predicted by the analysis when using the foreshock strong motion records, which is consistent with field observations.
3) Although some of the dynamic properties of the clay-like soil deposits were not available at the time of writing this paper, and therefore were inferred from the literature, the critical slip surface predicted for the main-shock event by the model closely resembled that observed at the landslide site. This shows that the assumptions made in regard to the clay-like deposits were acceptable.

The numerical simulation results suggest that the simultaneous pore pressure build-up and large inertial forces was likely the cause of the flow-type Takanodai slope failure. However, this could have led to two potential failure mechanisms: i) an abrupt flow-type failure (similar to that observed in monotonic undrained torsional shear test) or ii) a liquefaction-induced flow-type failure (similar to that observed in cyclic undrained torsional shear test). The numerical model used in this study was not able to differentiate between the two mechanisms. Therefore, Authors have planned to conduct additional advanced effective stress analyses using the state-dependent cyclic model for sand, known as UT-sand model (Chiaro et al., 2013 and 2017b) to confirm the most probable failure mechanisms for the Takanodai landslide.

This paper presents background information (including data, numerical model and descriptions) to help develop and inform discussions on the failure mechanism of the Takanodai landslide. The results of this study are not exhaustive and farther advanced numerical studies (e.g. effective stress analysis) are required before the actual Takanodai landslide failure mechanism can be confirmed.

ACKNOWLEDGEMENTS

The Authors would like to thank Associate Professor Takashi Kiyota and Mr. Muhammad Umar (University of Tokyo, Japan) for assisting with the field and laboratory investigations, and Dr Christopher Massey (GNS Science, NZ) and Mr. Claudio Cappellaro (University of Canterbury) for modelling insights. The First Author is grateful for the financial support from the New Zealand Society for Earthquake Engineering (NZSEE LFE Mission), the University of

Canterbury (UC CNRE Strategic Grant), and the Japan Science and Technology Agency (JST J-Rapid Kumamoto Project).

REFERENCES

1) Asadi, M.S., Asadi, M.B., Orense, R.P. and Pender, M.J. (2018): Undrained cyclic behavior of reconstituted natural pumiceous sands. Journal of Geotechnical and Geoenvironmental Engineering, ASCE, 114(8): 04018045.
2) Chiaro, G., Alexander, G., Brabhaharan, P., Massey C., Koseki J., Yamada, S. and Aoyagi, Y. (2017a): Reconnaissance report on geotechnical and geological aspects of the 2016 Kumamoto Earthquake, Japan. Bulletin New Zealand Society for Earthquake Engineering, 50(3): 365-393.
3) Chiaro, G., De Silva, L.I.N., and Koseki J. (2017b). Modeling the effects of static shear on the undrained cyclic torsional simple shear behavior of liquefiable sand. Geotechnical Engineering Journal, SEAGS, 48(4): 1-9.
4) Chiaro, G., Kiyota T., Pokhrel, R.M., Goda, K., Katagiri, T. and Sharma, K. (2015): Reconnaissance report on geotechnical and structural damage caused by the 2015 Gorkha Earthquake, Nepal. Soils and Foundations, 55(5): 1030-1043.
5) Chiaro, G., Koseki, J. and De Silva, L.I.N. (2013). A density- and stress-dependent elasto-plastic model for sands subjected to monotonic torsional shear loading. Geotechnical Engineering Journal, SEAGS, 44(2): 18-26.
6) Chiaro, G., Umar, M., Kiyota T. and Massey C. (2018): The Takanodai landslide, Kumamoto, Japan: insights from post-earthquake field observations, laboratory tests and numerical analyses. Proc. of the 5th Geotechnical Earthquake Engineering and Soil Dynamics Conference, June 10-13, Austin, Texas, USA (ASCE Geotechnical Special Publication, 293: 98-111).
7) Chigira, M. and Suzuki, T. (2016): Prediction of earthquake-induced landslides of pyroclastic fall deposits. Landslides and Engineered Slopes. Experience, Theory and Practice. Aversa, S., Cascini, L., Picarelli, L. and Scavia, C. (Eds.), CRC Press, 93-100.
8) Ishihara, K. and Harada, K. (1996): Cyclic behavior of partially saturated collapsible soils subjected to water permeation. Ground Failures under Seismic Conditions, ASCE, GSP 44: 34-50.
9) Dang, K., Sassa, K., Fukuoka, H., Sakai, N., Sato, Y., Takara, K., Quang, L.H., Loi, D.H., Tien, P.V. and Ha, N.D. (2016): Mechanism of two rapid and long runout landslides in the 16 April 2016 Kumamoto earthquake using a ring-shear apparatus and computer simulation (LS-RAPID). Landslides, 13(6): 1525–1534.
10) Dellow, S., Massey, C., Cox, S., Archibald, G., Begg, J., Bruce, Z., Carey, J., Davidson, J., Della Pasqua, F., Glassey, P., Hill. M., Jones, K., Lyndsell, B., Lukovic, B., McColl, S., Rattenbury, M., Read, S., Rosser, B., Singeisen, C., Townsend, D., Villamor, P., Villeneuve, M., Wartman, J., Rathje, E., Sitar, N., Adda, A.Z., Manousakis, J. and Little, M. (2017). Landslides caused by the Mw7.8 Kaikoura Earthquake and the immediate response. Bulletin New Zealand Society for Earthquake Engineering, 50(2): 106-116.
11) Goto, H., Hata, Y., Yoshimi, M. and Yoshida, N. (2017): Nonlinear site response at KiK-net KMMH16 (Mashiki) and heavily damaged sites during the 2016 Mw 7.1 Kumamoto Earthquake, Japan. Bulletin of the Seismological Society of America, 107(4): 1802-1816.
12) Hyodo. M., Hyde, A.F.L. and Aramaki, N. (1998): Liquefaction of crushable soils. Geotechnique, 48(4): 527-543.
13) Kiyota, T., Ikeda, T., Konagai, K. and Shiga, M. (2017). "Geotechnical damage caused by the 2016 Kumamoto Earthquake, Japan. International Journal of Geoengineering Case Histories, 4(2): 78-95.
14) Kramer, S.L. (1996). Geotechnical Earthquake Engineering. Prentice Hall, NJ, USA, pp. 653.
15) Lee, K.L. and Albaisa, A. (1974): Earthquake induced settlements in saturated sand. Journal of the Geotechnical Engineering Division, ASCE,, 100(GT4): 387-406.
16) Lee, K.L., Seed, H.B., Idriss, I.M. and Makdisi, F.I. (1975): Properties of soil in the San Fernando hydraulic fill dams. Journal of the Geotechnical Engineering Division, ASCE, 101(8): 801–821.
17) Meyer, V., Larkin, T. and Pender, M. (2005): The shear strength and dynamic shear stiffness of some New Zealand volcanic ash soils. Soils and Foundations, 45(3): 9–20.
18) Mukunoki, T., Kasama, T., Murakami, S., Ikemi, H., Ishikura, R., Fujikawa, T., Yasufuka, N. and Kitazono, Y. (2016): Reconnaissance report on geotechnical damage caused by an earthquake with JMA seismic intensity 7 twice in 28h, Kumamoto, Japan. Soils and Foundations, 56(6): 947-964.
19) Pender, M.J., Wesley, L.D., Larkin, T.J. and Pranjoto, S. (2006): Geotechnical properties of a pumice sand. Soils and Foundations, 46(1): 69-81.
20) Quake/W (2014): Dynamic Modeling with Quake/W. An engineering methodology. October 2014 Edition, GEO-SLOPE International Ltd., pp. 173.
21) Seed, H.B. and Idriss, I.M. (1971). Simplified procedure for evaluating soil liquefaction potential. Journal of the Soil Mechanics and Foundations Division, ASCE, SM(9): 1249-1273.
22) Slope/W (2012): Stability modelling with Slope/W. An engineering methodology. July 2012 Edition, GEO-SLOPE International Ltd., pp. 246.
23) Umar, M., Chiaro, G. and Kiyota T. (2017): Monotonic and cyclic undrained torsional shear behavior of Aso pumice soil. Bulletin of Earthquake Resistant Structure Research Center, Institute of Industrial Science, University of Tokyo, 50: 1-10.
24) Umar, M., Chiaro, G., Takashi K. and Miyamoto H. (2018): Monotonic and cyclic undrained behavior of Kumamoto-Aso pumice soil by triaxial and torsional shear tests. Proc. of the 16th European Conference on Earthquake Engineering, Thessaloniki, Greece.
25) Wang, G (2017): "Fluidized landsliding phenomena during earthquakes". Proc., JTC1 Workshop on Advances in Landslide Understanding, Barcelona, Spain, pp. 4.
26) Wesley, L. D. (2001): Determination of specific gravity and void ratio of pumice materials. Geotechnical Testing Journal, ASTM, 24(4): 418–422.
27) Yamanouchi, T. (1968): Ground failure due to the Ebino earthquake. Report of the JSSMFE Technical Committee on Shirasu. Tsuchi-to-kiso JSSMFE, 16(9): 47-59.
28) Yin, Y., Wang, F. and Sun, P. (2009): Landslide hazards triggered by the 2008 Wenchuan earthquake, Sichuan, China. Landslides, 6(2): 139–152.